Electronic structure of pure and defective $PbWO_4$, $CaWO_4$, and $CdWO_4$

R. T. Williams, Y. C. Zhang, Y. Abraham, and N. A. W. Holzwarth

Department of Physics, Wake Forest University
Winston-Salem, NC 27109 USA

Within the framework of density functional theory, we have studied the electronic ground-state properties and approximated the optical dielectric constants and reflectivity of $PbWO_4$ as well as $CaWO_4$ and $CdWO_4$. The band structure also provides insight into the transport properties of excitons, electrons, and holes in these materials. A supercell adaptation of our calculation method which was previously applied to $CaWO_4$:Pb at 50% concentration has now been used to study Pb vacancies, Bi impurities, and La impurities in $PbWO_4$. Preliminary results of electronic structure calculations for $CdWO_4$, having the wolframite structure, are presented for comparison.

Keywords: $PbWO_4$, $CaWO_4$, $CdWO_4$, electronic structure, defects

Introduction

Lead tungstate ($PbWO_4$) and cadmium tungstate ($CdWO_4$) are dense, fast scintillator crystals which have achieved technological importance for high energy radiation detectors and medical imaging, respectively. Calcium tungstate ($CaWO_4$, the mineral scheelite) is an important phosphor for lighting and displays. We recently compared the electronic structures of the four scheelite-structure materials $CaWO_4$, $PbWO_4$, $CaMoO_4$, and $PbMoO_4$ [1]. The present paper discusses further aspects of the electronic properties of the first two of these crystals and presents new electronic structure results for $CdWO_4$ using the same calculation method. Furthermore, a supercell adaptation of the method has been employed to study chemical impurities and vacancies at effective 50% concentrations. Results for Pb impurities in $CaWO_4$ were reported in Ref. [2]. Additional results on Pb vacancies, La impurities, and Bi impurities in $PbWO_4$ are reported here. Comparisons to experimental data on photoelectron spectroscopy, reflectivity [3], electronic transport, EPR, and luminescence spectroscopy will be discussed.

The density functional calculations were performed using the Linearized Augmented Plane Wave (LAPW) technique using the WIEN97 code[4]. The calculational and convergence parameters were detailed in our previous work[1-3].

One electron energy spectrum of $PbWO_4$

The density of states (*N(E)*) distribution for $PbWO_4$ from -20 to +15 eV is presented in Fig. 1. The labels appearing above the peaks indicate the dominant atomic and molecular

attributes of each band, determined by analyzing the partial densities of states and contour maps of the electron densities for specific energy ranges [1] as will be discussed below. Recently, Hofstaetter, Meyer, Niessner, and Oesterreicher[5] have measured the ultraviolet photoelectron spectrum (UPS) of $PbWO_4$ which is also shown in Fig. 1. The energy scale of the UPS has been translated rigidly for best agreement of major features of the calculation. In particular, the spectrum can be made to align simultaneously with the "Pb6s-O2p" peak, the bottom of the valence band, the two main groups of oxygen states in the valence bands, and the valence band edge. This alignment of energy scales corresponds to a value of photoelectron threshold energy (from top of valence band to vacuum energy) of 5 eV. This is a reasonable value corresponding to the sum of the 4.2 eV band gap and a small positive electron affinity. On the other hand, photoelectron spectra measured by Shpinkov et al show at most a small bump in the place expected for the Pb6s-O2pσ band below the valence band. [6]

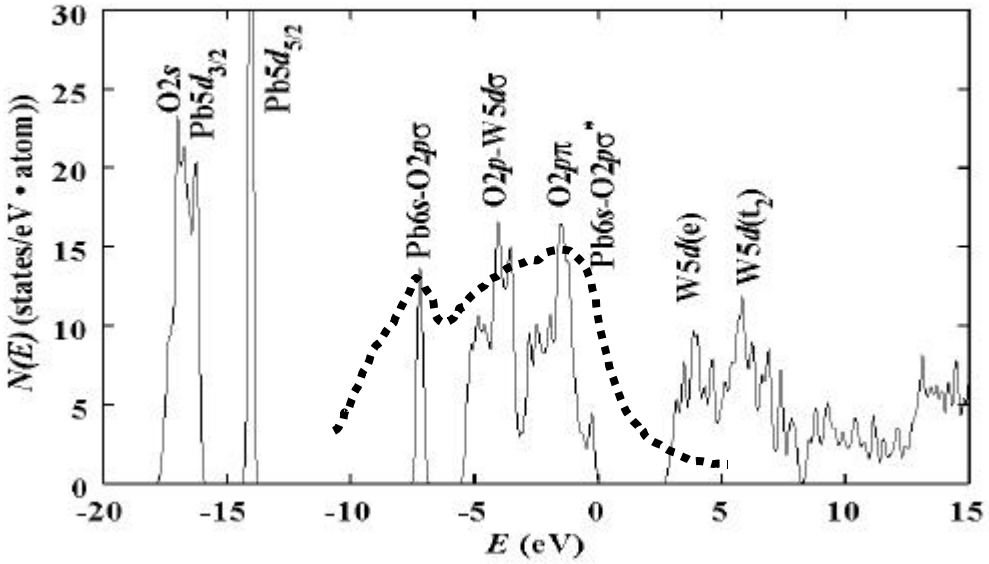

Fig. 1 -- Total density of states for the upper core, valence, and conduction bands of $PbWO_4$ calculated with a Gaussian smearing function (Ref. [1,3]). The zero of energy is taken at the top of the last occupied band. The labels indicate the dominant atomic and molecular attributes of each band. The broken curve is an experimental ultraviolet photoelectron spectrum from Hofstaetter et al [5] as discussed in the text.

For the scheelite materials, the structure of *N(E)* in the vicinity of the band gap is primarily associated with the WO_4 group which has approximately tetrahedral symmetry. A molecular orbital diagram for these states, based on the work of Ballhausen [7] and from analysis of the electronic structure results, is shown in Fig. 2. The W^{6+} ions split the 2*p* states of the nearest neighbor O^{2-} ions into σ and π orbitals. These states then form linear combinations appropriate for the tetrahedral symmetry of the WO_4 site to compose the main contribution to the valence bands. The 5*d* states of the W^{6+} ions also hybridize with the O 2*p* states and the tetrahedral crystal field splits the *5d* orbitals into "e" states which dominate the bottom of the conduction band and the "t_2" states which dominate the

upper conduction band. This basic structure is also seen in the density of states for $CaWO_4$. In addition, the valence band of $PbWO_4$ is also strongly affected by the Pb 6*s* states which hybridize with the O 2*p* states in an approximately octahedral environment, as also diagrammed in Fig. 2. The "Pb6*s*—O2*p*σ" hybrid forms a bonding state *below* the bottom of the valence band while the "Pb6*s*—O2*p*σ^*" antibonding hybrid contributes to the density of states at the top of the valence band of $PbWO_4$.

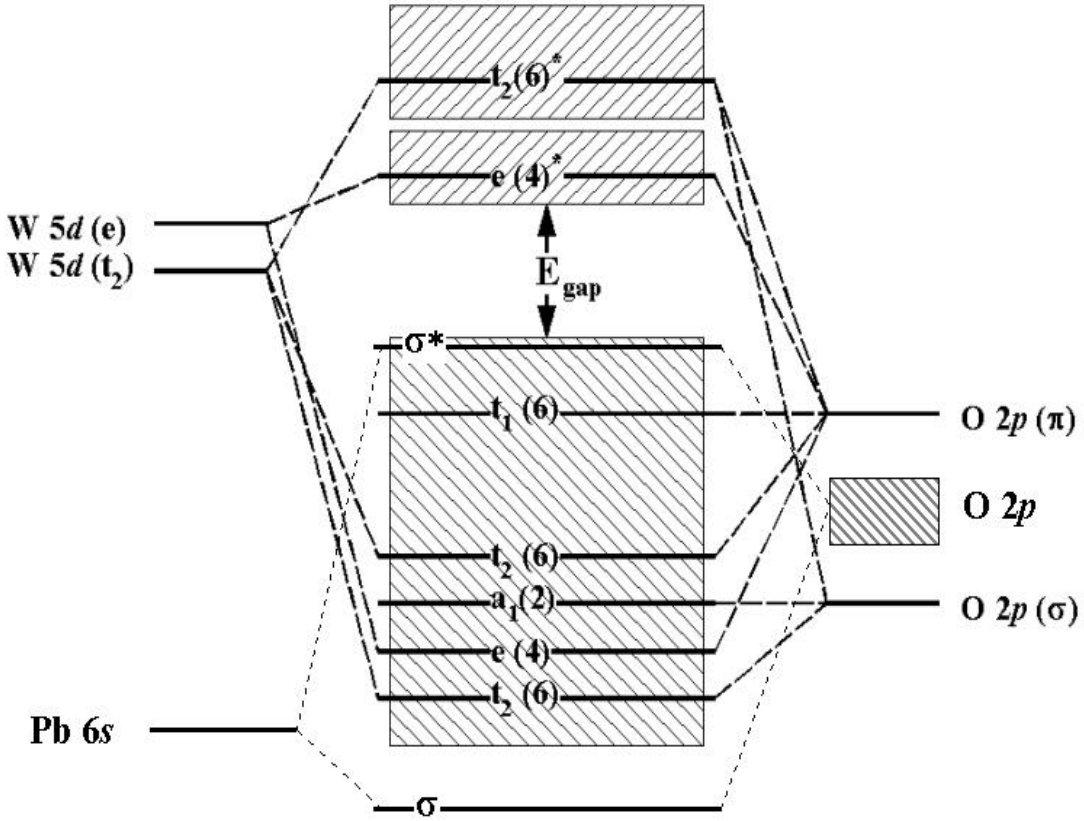

Figure 2. Schematic molecular orbital diagram for W-O and Pb-O interactions superimposed on blocks representing calculated $PbWO_4$ valence and conduction bands.

Experimental confirmation of the Pb6s-O2p character of states at the top of the valence band of $PbWO_4$ can be inferred from consideration of EPR studies of Pb impurity states in $CaWO_4$ by Born, Hofstaetter, and Scharmann [8]. Analysis of the EPR hyperfine analysis showed that $CaWO_4$:Pb exhibits a shallow hole state centered on Pb with approximately 50/50 sharing of the hole between Pb6*s* and the O2*p* ligands [8]. This is in qualitative agreement with the calculated partial densities of states found in a supercell simulation of $CaWO_4$: $PbWO_4$ alloy (at 50% concentration) by the present method [2]. Thus, there are several experimental results which are consistent with our analysis of the role of bonding and antibonding Pb6*s*--O2*p* states in pure $PbWO_4$.

Band dispersion, self-trapping, geminate recombination

The energy dispersion curves of $PbWO_4$ and $CaWO_4$ are compared in Fig. 3. The minimum band gap in $CaWO_4$ is at Γ, whereas in $PbWO_4$ the minimum gap is definitely away from Γ, apparently indirect from Δ to Σ with direct gaps at Δ and Σ lying only

slightly higher.[1] The main reason for this difference in the nature of the two band gaps is the highly dispersing band at the top of the valence bands, derived from the Pb6*s*—O2*p* antibonding state discussed above. The band structures in Fig. 3 provide a reasonable basis for understanding what has heretofore been a puzzling mixture of experimental differences and similarities between the two scheelite-structure tungstates $CaWO_4$ and $PbWO_4$, namely:

(a) Self-trapped holes in $CaWO_4$ are observable by EPR with stability up to 150K [9], whereas no EPR of self-trapped holes has been observed in $PbWO_4$ at any temperature.[10] The data in $CaWO_4$ show that the hole autolocalizes on a relaxed pair of (WO_4^{2-}) tungstate groups.[9]

(b) In fact, no significant concentrations of trapped holes in any paramagnetic sites are found in $PbWO_4$ irradiated at low temperature. Yet trapped electron centers including intrinsic self-trapped electrons (see below) are found in $PbWO_4$, so holes reside somewhere, presumably in nonparamagnetic pairings. [11]

(c) Electrons self-trap on an intrinsic tungstate group as WO_4^{3-} in $PbWO_4$, observed by EPR with stability up to 50 K.[12,13] In $CaWO_4$, electrons localize on a tungstate group perturbed by a defect on the neighbor cation site.[9]

(d) The intrinsic blue recombination luminescence in both $CaWO_4$ and $PbWO_4$ has many experimental similarities, and is attributed in both cases to electron-hole recombination on a local tungstate group of the perfect crystal, i.e. a self-trapped exciton on the tungstate sublattice. [14] This similarity of the recombination event in the two materials contrasts with the difference in hole trapping.

Considering the $CaWO_4$ band structure in Fig. 3 and the previous accompanying discussion, we see that the W-O2pπ states at the top of the valence band, to which holes would relax before self-trapping, have narrow dispersion width of about 0.5 eV per band. The empirical fact that holes self-trap in $CaWO_4$ is at least consistent with the narrow dispersion of the topmost valence band. As discussed by Toyozawa [15], a carrier in a band will self-trap if the local lattice relaxation energy it induces, E_{LR}, exceeds the localization energy equal to half the dispersion width of the band, W/2. Their difference is the thermal trap depth, E_T, of the autolocalized carrier. Herget et al [9] determined that E_T = 0.42 eV for self-trapped holes in $CaWO_4$.

In $PbWO_4$, the similar narrow tungstate energy bands are present near the top of the valence bands, but the dispersive Pb-O band extends 1 eV higher than the tungstate bands. A hole will move from the tungstate groups up into the Pb-O band on a time scale much shorter than needed for self-trapping. Because of the 1-eV width of the Pb-O band, the cost of hole localization from that band is approximately a factor of two higher than in the topmost tungstate valence band. Thus, the single-particle band-structure supports the empirical observation that individual holes in $PbWO_4$ are mobile whereas holes autolocalize in $CaWO_4$. The mobile holes in $PbWO_4$ may find diamagnetic trapping centers or possibly pair into 2-hole singlet self-trapped states of unknown structure.

In view of this difference of hole-trapping in the two materials, what can we understand of the strong similarity of blue recombination luminescence attributed to an exciton autolocalized on the tungstate group in both crystals? It suggests that excitons but not holes self-trap on the tungstate sublattice in $PbWO_4$. There is a well documented precedent for just this behavior in alpha quartz (SiO_2), where excitons are well known to self-trap, but stable self-trapped holes are not found.[16] The fact that the electron self-

traps in $PbWO_4$ implies that its interaction with the lattice will contribute to exciton localization. The fact that the electron is known to autolocalize on a tungstate group, not on Pb-O bonds, suggests how it may "anchor" the exciton to a particular tungstate group and so prevent dissipation of the hole wavefunction along the Pb-O valence states.

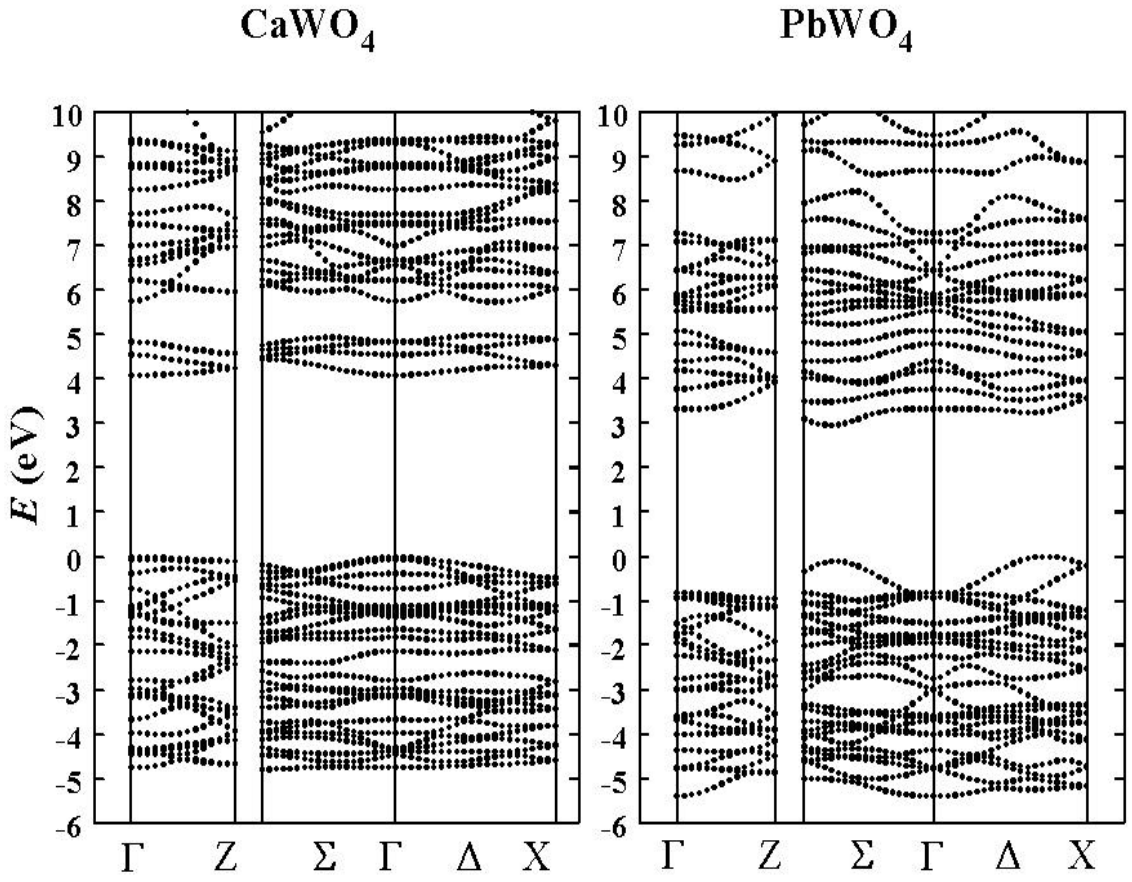

Figure 3. Energy dispersion curves for $CaWO_4$ and $PbWO_4$.

Another difference in the band structures of $CaWO_4$ and $PbWO_4$ which is noticeable in Fig. 3 is that the conduction bands of $CaWO_4$ clearly divide into two groups with a gap of nearly 1 eV between, whereas there is not such a clear division nor a gap in the $PbWO_4$ conduction bands. The lower conduction bands in $CaWO_4$ are composed mainly of W states, whereas the upper group of conduction bands has strong Ca3d character, as previously noted. The conduction bands of $PbWO_4$ have strong W character throughout, with weak hybridization of Pb states. The conduction band character of $CaWO_4$ provides a reasonable basis for understanding the unusually large 2.2 eV difference between the band gap of $CaWO_4$ and the threshold for excitation of thermoluminescence (i.e. production of free carriers which escape geminate recombinaton). [17, 18] Electrons excited to the lower conduction band and holes in the valence band quickly relax to self-trapped excitons and undergo geminate recombination, yielding intrinsic blue luminescence in pure crystals. This route successfully competes with the escape of carriers to defect traps that can be seen in thermoluminescence; hence, the absence of thermoluminescence excitation in the corresponding photon energy range.[17,18]

However, photons of energy 2 or 3 eV higher than the band edge can excite electrons into the Ca3d conduction band. Existence of the 1-eV gap retards their scattering into the lower conduction states that contribute to bound exciton states, allowing free-electron transport to charge traps and corresponding thermoluminescence, as observed.

In $PbWO_4$, the offset between the band gap (actually the lowest reflectivity peak) and the threshold of thermoluminescence excitation is smaller, about 0.7 eV. However, this is much larger than the probable exciton binding energy (< 0.1 eV, see below). In Ref. [3], we described a model in which the geminate recombination yield is greatest for excitation of carriers just to the band edges, where electrons are known to autolocalize in $PbWO_4$. Under the reasonable assumption that polaron mobility becomes higher in states farther from the band edges, non-geminate carrier processes eventually become dominant as the band-to-band excitation energy is raised. The threshold of their dominance is the threshold for thermoluminescence excitation.

Optical constants, reflectivity, and exciton binding energy

Although density functional theory is rigorously a ground-state formalism, there has recently been considerable progress in developing methods to calculate optical properties using density functional results as the starting point [19]. As a first step toward investigating the optical properties, we have calculated the imaginary part of the dielectric constant from the self-consistent LAPW wavefunctions $y_{nk}(\boldsymbol{r})$ and one-electron eigenvalues E_{nk}, using the code developed by Abt and Ambrosch-Draxl [20]. There are of course no excitonic effects included in these calculations. Taking the Kramers-Kronig transform of ε_2, we obtain the calculated spectrum of ε_1 after adjusting the calculated band gap and calculated visible refractive index to agree with experiment. [21] Our calculated reflectivity was compared to the experimental measurement by Shpinkov *et al* [22] in Refs. [2,3]. The agreement between the measured and calculated reflectivity for $PbWO_4$ is surprisingly good. The sharp peak in the calculated spectrum at the band edge is due to a near singularity in the joint density of single-particle states. Since no lower-energy discrete features are found in the experimental spectrum, we conclude that whatever exciton discrete states are observable in the absorption spectrum should have a low binding energy compared to the ~0.3 eV width of the experimental reflectivity peak. The suggestion of a small exciton binding energy in $PbWO_4$ was supported by consideration in Ref. [3] of the measured optical and static dielectric constants for $PbWO_4$ which are quite large -- $\varepsilon_1(1.9\text{ eV}) \equiv \text{å}_{opt} = 5.06$ [21] and $\varepsilon_1(0\text{ eV}) \equiv \text{å}_{static} = 23.6$, respectively, for a-axis polarization.

Defects and dopants

Defects and dopants in the tungstate crystals have been studied using the present calculation method adapted for a supercell of two normal unit cells, in one of which the imperfection is introduced. The defects studied in this way are effectively at 50% alloy composition. The method and results for $CaWO_4$:Pb were described in Ref. [2]. In the present paper, we report results obtained in this way for Pb vacancies, Bi impurity substituting for Pb, and La impurity substituting for Pb in the $PbWO_4$ crystal. Figure 4 shows the valence and conduction band partial density of states curves for each of the three defects alongside the partial DOS for perfect $PbWO_4$. Lattice relaxation around the defects has not yet been included in these results.

Pb vacancy -- Pb vacancies in $PbWO_4$ are hole traps considered important in radiation damage and charge transport. [10,11] In the case illustrated in Fig. 4, removal of 50% of the neutral Pb atoms from the crystal leaves it noticeably electron deficient, with the Fermi level moving about 0.5 eV below the top of the valence band. There are no new states introduced deep in the gap. The conduction band edge states seem somewhat more separated from the main conduction band in the crystal with vacancies, but it is not clear that a gap state has split off from the conduction band. As expected from doubling of the unit cell size, the bands are narrower in the crystal with periodic vacancies, and charge becomes more localized on the Pb6s-O2p bonding state. The top of the valence band has a stronger Pb-O character in the defective than in the perfect crystal, implying that holes will exist largely on oxygen and on the Pb ions neighboring the Pb vacancy. The calculation confirms the experimental evidence [10,11] that Pb vacancies do not introduce a deep mid-gap trap, but rather a shallow acceptor level.

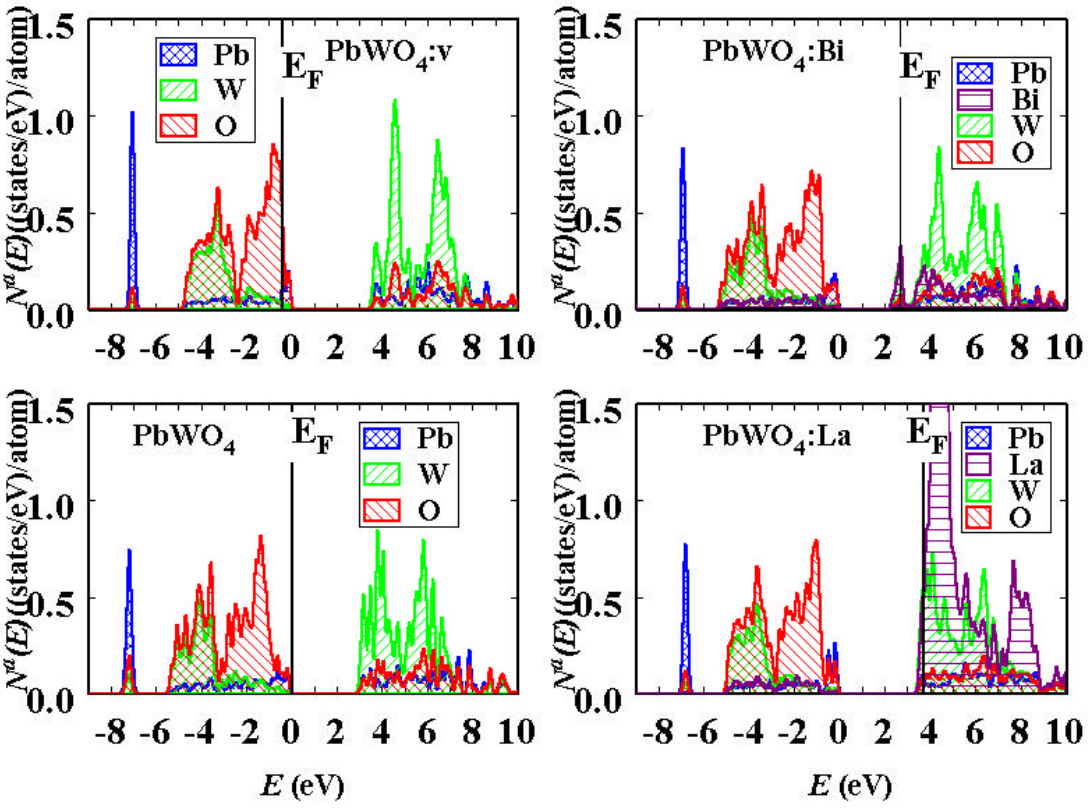

Figure 4. Partial densities of states data calculated for pure $PbWO_4$, Pb vacancies "$PbWO_4$:v", and Bi and La substitutional impurities ("$PbWO_4$:Bi" and "$PbWO_4$:La", respectively). The defects are effectively at 50% concentration, calculated in a supercell adaptation of the LAPW method used for pure $PbWO_4$. The Fermi levels are marked as E_F and the zero of energy is taken to be at the top of the oxygen bands.

$PbWO_4$:Bi --Bismuth has one higher atomic number than Pb, and so should act as a donor when substitutionally incorporated in $PbWO_4$. Using the same supercell approach, every alternate Pb was replaced by Bi. The partial DOS plot is shown in Fig.4. A distinct, partially filled band occurs in the upper band gap. It is not simply composed of

Bi states, but has a nearly equal contribution from W ions, forming the localized gap state.

$PbWO_4$:La -- Lanthanum ionizes to La^{3+} when substituted for Pb in the $PbWO_4$ host, contributing an extra electron per La atom incorporated. The Fermi level lies in the bottom of the conduction band for this 50% alloy composition. The DOS shoulder at the top of the valence band in Fig. 4 seems enhanced with La incorporated. There is a very strong DOS contribution from La in the lower conduction band states. Note that in contrast to Bi, the La dopant acts as an electron donor without simultaneously introducing a new state in the band gap. This agrees with experimental observations on the role of La dopant in $PbWO_4$, which is that it has the beneficial effect of donating electrons to fill potential hole traps and thus improve post-radiation transparency, without itself introducing absorption bands that adversely affect transparency. The La contribution to the valence bands is f-like in the intense lower peaks, and d-like in the peaks at higher energy.

Cadmium tungstate, $CdWO_4$

Band structure calculations for $CdWO_4$ (having wolframite structure) and $CdMoO_4$ (having scheelite structure) have recently been undertaken using the same calculation method. The detailed results will be presented in a future publication, but because of the importance of cadmium tungstate as a medical imaging scintillator and basic interest in comparing a tungstate crystal having wolframite structure with results on scheelite structure discussed above, we would like to briefly present some of the preliminary results here. In the wolframite structure, oxygen ions are arranged with 3 different bond lengths in approximately octahedral symmetry around the tungsten ions, in contrast to the 4 equal bond lengths in nearly tetrahedral symmetry of oxygens around tungsten in the scheelite materials such as $CaWO_4$ and $PbWO_4$. Oxygen has an approximate octahedral arrangement around Cd sites in $CdWO_4$, roughly as it does around Ca and Pb in the respective scheelite tungstates.

The partial density of states plot for the valence and conduction bands is shown in Fig. 5. Oxygen 2*p* states dominate the top of the valence band, with some contribution from Cd, but very little from W. The bottom of the valence bands is dominated by Cd 4*d* states, while the middle of the valence band has some W 5*d* contribution. It is noticeable that the valence bands do not exhibit the clear grouping into O2$p\sigma$ bonding and O2$p\pi$ nonbonding combinations with tungsten as was seen in $CaWO_4$ and $PbWO_4$. That basic structure still characterizes the valence band to be sure, but perhaps because of the lower symmetry, the notch of demarcation between the two groups is not evident for $CdWO_4$. While Cd-O orbitals are dominant at the top of the valence band, there is no indication of a Cd-O band isolated from the W-O bands as was found in $PbWO_4$.

The conduction bands group into two regions derived primarily from the W 5*d* states, the lower band is derived from "t_2" molecular orbitals while the upper band is derived from "e" orbitals. It is interesting that this is the reverse of the ordering of conduction band states found in the scheelite crystals studied previously. That is, in $CaWO_4$ and $PbWO_4$, the "e" states comprise the lower conduction bands and the t_2 states the upper. This reversal can be explained by the following symmetry considerations. In both the wolframite and scheelite tungstates, the conduction band is dominated by the crystal field

split W 5*d* orbitals with the weakly bonding state forming the lower conduction band and the more strongly antibonding state forming the upper conduction band. In the octahedral geometry (wolframite structure), the "t_2" orbitals are approximately directed *between* the

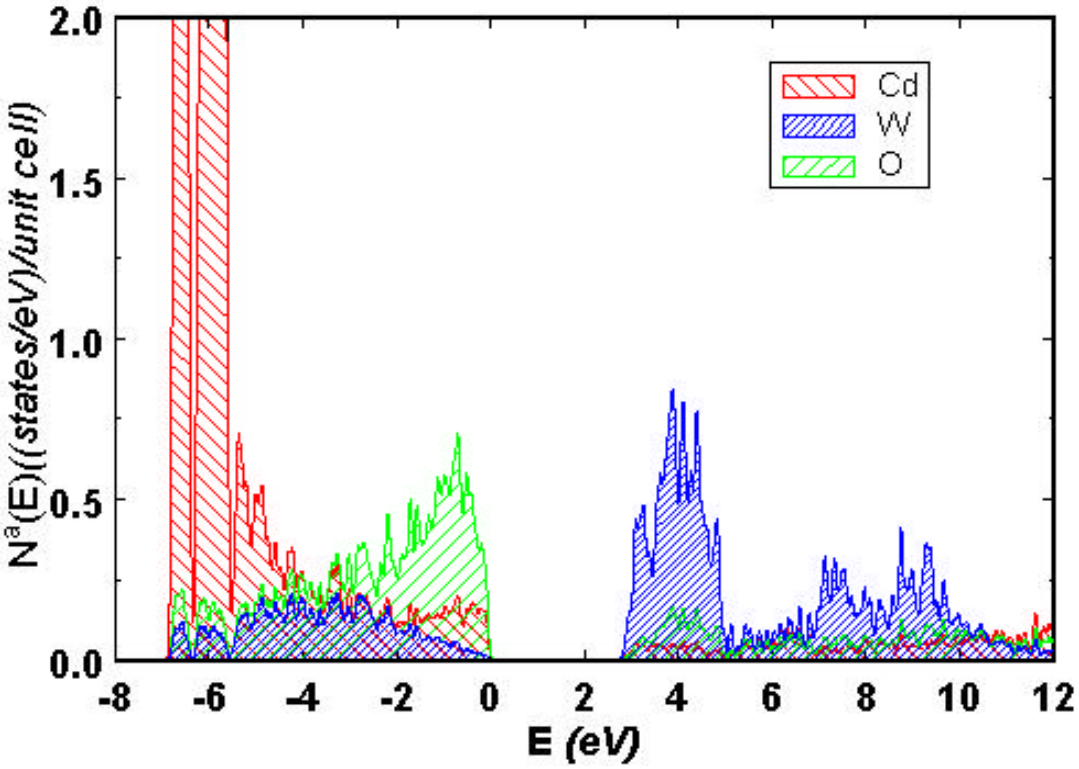

Figure 5. $CdWO_4$ partial densities of states.

bond directions while "e" orbitals are approximately directed *along* the bond directions. In the tetrahedral geometry (scheelite structure), the "e" orbitals are approximately directed *between* the bond directions while "t_2" orbitals are approximately directed *along* the bond directions. Nagirnyi has also concluded from polarization of the intrinsic luminescence that the ordering of the e and t_2 conduction states is reversed in $CdWO_4$ relative to $PbWO_4$.[23]

The energy dispersion curves calculated for $CdWO_4$ cannot be presented here for lack of space. They show that the minimum band gap does not occur at Γ but at Y, which is at the zone face center along the b crystal axis. The top of the valence band has narrow dispersion. The lowest conduction band has relatively wide dispersion relative to the tungstate crystals considered previously. The preliminary calculated reflectivity spectrum of $CdWO_4$ has only a broad peak above the band edge, in contrast to the sharp structure of $PbWO_4$ reflectivity, but in approximate agreement with the experimental observation of only very weak reflectivity structure above the band edge of $CdWO_4$.[18]

Acknowledgments

We acknowledge support by NSF grants # DMR-9403009, -9706575, and -9732023. We would like to thank A. Hofstaetter, M. Nikl, and N. Nagirnyi for helpful discussions and sharing of unpublished data.

References

1. Y. Zhang, N. A. W. Holzwarth, and R. T. Williams, Phys. Rev. B **57**, 12738 (1998).
2. N. A. W. Holzwarth, Y. Zhang, and R. T. Williams, International Workshop on Tungstate Crystals, Roma, October 12-14, 1998.
3. Y. C. Zhang, N. A. W. Holzwarth, R. T. Williams, and M. Nikl, Proc. 3rd Int'l Conf. on Excitonic Processes in Condensed Matter, ed. by R. T. Williams and W. M. Yen (The Electrochemical Society, Pennington, N. J., 1999) p. 420.
4. P. Blaha, K. Schwarz, and J. Luitz, WIEN97, Vienna University of Technology, 1997 [Improved and updated Unix version of the orginal copyrighted WIEN code, which was published by P. Blaha, K. Schwarz, P. Sorantin, and S. B. Trickey, Comput. Phys. Commun. **59**, 399 (1990)].
5. A. Hofstaetter, B. K. Meyer, W. Niessner, and I. Oesterreicher, private communication.
6. I. A. Shpinkov, I. A. Kamenskikh, V. N. Kolobanov, and V. V. Mikhailin, CMS Document 1996-213, 2nd Annual RDMS CMS Collaboration Meeting, CERN, Dec. 16-17, 1996 (unpublished).
7. C. J. Ballhausen and A. D. Liehr, J. Mol. Spectrosc. **2**, 342 (1958).
8. G. Born, A. Hofstaetter, and A. Scharmann, Z. Physik **245**, 333 (1971).
9. M. Herget, A. Hofstaetter, T. Nickel, and A Scharmann, Phys. State. Sol. (b) **141**, 523 (1987).
10. S. Baccaro et al, Proc. Intl. Workshop on Tungstate Crystals, Rome, Oct. 1998.
11. A. Annenkov, E. Auffray, M. Korzhik, P. Lecoq, and J. –P. Peigneux, phys. stat. sol. (a) **170**, 47 (1998).
12. V. V. Laguta, J. Rosa, M. I. Zaritskii, M. Nikl, and Y. Usuki, J. Phys. Cond. Matter **10**, 7293 (1998).
13. Böhm, F. Henecker, A. Hofstaetter, M. Luh, B. K. Meyer, O. V. Kondratiev, and M. V. Korzhik, Proc. of European Conference on Defects in Insulating Materials, EURODIM98, Keele, UK, July 6-11, 1998.
14. S. G. Nedel'ko et al, in Proc. of SCINT95 (Delft University Press, Delft, 1996) 263.
15. Y. Toyozawa: Electrons, holes, and excitons in deformable lattice, in *Relaxation of Excitations*, Springer Ser. Solid State Sci., Vol. 18, ed. By R. Kubo, E. Hanamura (Springer, Berlin, Heidelberg, 1980), p. 3.
16. W. Hayes, M. H. Kane, O. Salminen, R. L. Wood, and S. P. Doherty, J. Phys. C **17**, 2943 (1984); W. Hayes and T. J. L. Jenkin, J. Phys. C **19**, 6211 (1986); K. S. Song and R. T. Williams, Self-Trapped Excitons, Springer Ser. In Solid State Sci., Vol 105 (Springer, Berlin, Heidelberg, 1993) p. 293.
17. V. Mürk, M. Nikl, E. Mihokova, and K. Nitsch, J. Phys.: Condens. Matter 9, 249 (1997).
18. V. Nagirnyi, E. Feldbach, L. Jönsson, M. Kirm, A. Kotlov, A. Lushchik, L.L. Nagornaya, V. D. Ryzhikov, G. Svensson, I. A. Tupitsina, M. Åberg-Dahl, Proc. Workshop on $PbWO_4$, Rome, Oct. 12-15 (1998).
19. R. Del Sole and R. Girlanda, Phys. Rev. B **48**, 11789 (1993); M. Rohlfing and S. G. Louie, Phys. Rev. Lett. **81**, 2312 (1998).
20. R. Abt, C. Ambrosch-Draxl, and P. Knoll, Physica B **194-195**, 1451 (1994).
21. G.F.Bakhshieva and A.M.Morozov, Sov.I.Opt.Technol. **44**(9), 542 (1977).
22. I. N. Shpinkov, I. A. Kamenskikh, M. Kirm, V. N. Kolobanov, V. V. Mikhailin, A. N. Vasil'ev, and G. Zimmerer, phys. stat. sol. (a) **170**, 167 (1998).
23. V. Nagirnyi, International Conference on Luminescence, Osaka, August 23-27, 1999.